Desalination and Water Treatment
www.deswater.com
doi: 10.5004/dwt.2020.26052

198 (2020) 71–79
September

Mineral particles fouling analysis and cleaning in seawater reverse osmosis desalination

Wei Xue, Guochen Cheng, Yunfang Wu, Xiangyu Hou, Weizhen Wang, Jianhua Yin*

The Institute of Seawater Desalination and Multipurpose Utilization, MNR (Tianjin), 55 Hanghai RD, Tianjin 300192, China, emails: xuewei8035@163.com (W. Xue), chengguochen@163.com (G. Cheng), dhswyf@126.com (Y. Wu), houxiangyu020652@126.com (X. Hou), 13920481628@163.com (W. Wang), dhsyinjianhua@163.com (J. Yin)

Received 7 January 2020; Accepted 3 May 2020

ABSTRACT

Particles were the most frequent foulants in seawater reverse osmosis (SWRO) desalination. In this study, the fouling characteristic of particles in a large scale SWRO desalination plant from northern China was analyzed systematically by multiple methods. The particle fouling pattern, particle size distribution (PSD), and mineralogical composition were investigated by optical microscopy, scanning electron microscopy with energy dispersive spectrometer, laser diffraction particle size analyzer, X-ray diffraction, and wavelength dispersive X-ray fluorescence spectrometer. Chemical analysis indicated that Na, Mg, Si, and Al were the predominant elements contributing to the fouling particles. The particle deposition had a very broad PSD including ultrafine particles, fine particles, and medium particles due to the failure of the ultrafiltration (UF) system. The mineralogical components were quartz, muscovite, talc, albite, microcline, clinochlore, hematite, and amphibole in descending order. Finally, the long immersing experiment shows that 2.5% hydrofluoric acid processing could eliminate the particles effectively and improve the water flux of the fouled membrane obviously. On the basis of the above results, an in-depth understanding and mitigation of the particles fouling behavior during SWRO desalination would be put forward.

Keywords: Desalination plant; Reverse osmosis; Membrane fouling; Mineral particles; Chemical cleaning

1. Introduction

Seawater reverse osmosis (SWRO) desalination is one of the most reliable approaches to solve the problem of water shortage, especially in cities located in the coastal area [1,2]. According to the 2018–2019 International Desalination Association Water Security Handbook, 1.9 million m^3/d of seawater capacity was contracted in the first half of 2018, up 26% over the same period in 2017 [3,4]. The key feature of SWRO desalination is the ability to produce high-quality freshwater reliably by the effective rejection of salt in the feed. However, the membrane permeates quality would be reduced by fouling on the concentration side of the membrane [5–7], such as scaling [8,9], particles deposition, adsorption of organic matter [10,11], microorganism growth [12–14], and colloidal fouling [15,16]. Among the various foulant types, mineral particles in the feed cause severe problems during the reverse osmosis separation process because of clogging and physical damage, which is still an inevitable challenge to reliable seawater pretreatment [17,18].

Pretreatment processes like coagulation, dissolved air flotation, conventional granular media filtration, microfiltration (MF), ultrafiltration (UF), and cartridge filtration would remove particulate matters from the raw seawater [19–21]. UF processes are the most widely used pretreatment systems, which has been shown to be very effective for particulate foulants removal as well as for the removal of colloidal and biological fouling in the raw seawater.

* Corresponding author.

Nevertheless, the UF membrane fiber may be damaged by hypochlorite cleaning or high operating pressures, which results in particulate matter passing through the UF into the RO system. In practice, the particles are usually monitored by turbidity and silt density index (SDI). However, it is easy to ignore particulate pollution during the SWRO desalination, due to limited sensitivity of turbidity and poor reproducibility of SDI measurements for small changes in UF permeate quality [22,23].

Mineral particle is a class of natural fine-grained hydrated phyllosilicate minerals [24]. The particles are easy to deposit and form a cohesive cake layer on the surface of the membrane, resulting in various phenomena such as permeate flux reduction, salt passage increase, feed pressure increase, and membrane damage [17]. Once the particles fouling occurs in RO system, it is difficult to restore membrane performance by conventional cleaning, because they are chemically resistant, which is difficult to be dissolved by traditional chemical cleaning agent like hydrochloric acid and sodium hydroxide [25]. At the same time, these mineral particles will adsorb colloids, organic matter, or microorganisms in the seawater to form a dense mud cake, which will continuously deteriorate the membrane performance [26]. Finally, membrane autopsy has to be carried out in order to directly identify the main pollutants and optimize targeted pretreatment strategy.

Various qualitative and quantitative analytical methods, such as optical microscopy, scanning electron microscopy with energy dispersive spectrometer (SEM-EDS), transmission electron microscopy (TEM), Fourier transform infrared spectroscopy (FTIR), X-ray fluorescence (XRF), X-ray diffraction (XRD), inductively coupled plasma mass spectrometry (ICP-MS), atomic absorption spectroscopy (AAS), and ion chromatography (IC), laser light scattering and diffraction analysis, have been widely used to identify membrane foulants [27]. The reported membrane autopsy analysis usually focused on information such as foulants color, distribution morphology, cake thickness, chemical elements, and functional groups to diagnose the source and composition of the pollutant. This information is effective for some types of foulants analysis, but not enough for mineral particles. For the analysis of mineral particulate foulants, particle size distribution (PSD), and XRD analysis should be emphasized to determine the specific mineral species and structure to enable diagnosis of dominant fouling mechanism and optimize cleaning method.

Several studies have characterized mineral particles fouling in brackish water and wastewater [28–30], but there is no systematic report on mineral particles fouling in a large scale SWRO desalination plant. Meanwhile, recent studies are insufficient to ascertain the mineral cleaning methods for SWRO desalination.

In this work, the main object was to evaluate the particle components depositing on the RO membrane surface in order to provide valuable insight into the mineral particles fouling characteristics of SWRO desalination. The chemical composition, PSD, and mineralogical components of the particle foulants were analyzed and associated with feed water characteristics to figure out the source of contaminants, so as to allow us to discover membranes clogging of natural mineral particles and to select a properly designed pretreatment system allowing SWRO desalination plants to prolong the membrane useful life. Hydrofluoric acid (HF) cleaning agent was applied to dissolve the mineral particles to elucidate the effects of chemical cleaning to restore the performance of fouled SWRO membrane. The results of this study are expected to provide useful information on optimizing SWRO desalination plant operation.

2. Materials and methods

2.1. SWRO desalination plant

The fouled RO membrane was collected from a large scale SWRO desalination plant in north China that mainly supplies water for municipal and industrial use. The capacity of the full-scale plant was 80,000–100,000 m^3/d, at a 45% recovery rate, and was fed with seawater from Jiao Zhou Gulf through an open intake seawater lake. Fig. 1 shows a diagram of overview process in the SWRO desalination plant.

The pretreatment part only consisted of self-cleaning filters (Schunmann, F450) and ultrafiltration (UF) membranes (X-Flow SEAFLEX 55) with a nominal pore size of 20 nm. The ultrafiltration system controlled by an auto time-based backwash system according to the transmembrane pressure. The initial turbidity of seawater was 2–30 NTU, which was high, but was usually reduced to 0.05–0.5 NTU after ultrafiltration membrane processing. Self-cleaning filters would be fully blocked by silt-clay sediment during storm surges or algal blooms, which had to be cleaned through manual process by high-pressure water jet flushing. UF fouling followed by self-cleaning filters block resulted in higher transmembrane pressure and immediately flux decline. The feed seawater temperature ranges from 0°C–35°C with seasonal changes and the tested chemical compositions are presented in Table 1.

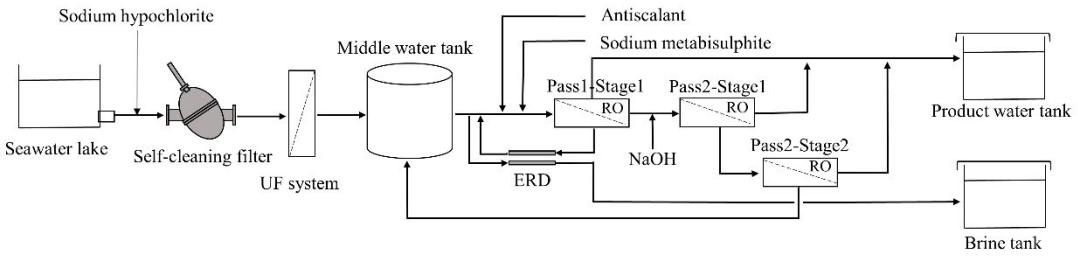

Fig. 1. Schematic diagram of major process in SWRO plant.

The seawater without pretreatment by coagulation, flocculation, or sedimentation was disinfected about 0.5 h every day at the head of intake pipe by sodium hypochlorite (about 2 mg/L) to control bacterial growth. After UF filtration, PWT Titan ASD 200 antiscalant (about 1.5 mg/L), which would not precipitate or bind to membranes at high concentrations, was used to inhibit $CaCO_3$ and $BaSO_4$ scaling of seawater during the RO membrane processing. Sodium metabisulfite was added to seawater in order to reduce residual chlorine and mitigate the membrane degradation.

If the transmembrane pressure increased to 3 bar, permeate flux or salt rejection drop significantly, chemical cleaning of RO membranes had to be carried out. The cleaning procedure normally included three stages in series: (1) biocidal cleaning with DBNPA (50 mg/L), (2) followed by alkaline cleaning with sodium hydroxide solution (pH = 12 ± 0.5), (3) followed by acid cleaning with hydrochloric acid (pH = 2 ± 0.5). This chemical cleaning did not achieve an obviously recovery of the initial performance of the RO membrane, despite prolonging the chemical cleaning times, and repeating frequency.

2.2. Membrane sampling

In this study, the last spiral wound RO element in pass1-stage1 pressure vessels was collected in October, 2018. The Manufacturer's recommended performances of RO membranes are shown in Table 2. The RO membranes had been worked unsteadily with low permeate flow and high pressure drop since year 2018. The fouled RO membrane modules were tested and autopsied immediately to minimize the change of constituents on RO membrane surfaces after collection.

Permeability and salt rejection of the fouled element were determined according to the procedure described by China industry standard HY/T 107-2017. The details of test results were provided in Table 3. Result showed that both salt rejection and normalized water flux of fouled RO element decreased significantly, compared with virgin element. The standard element test had a 23.44% reduction in water flux and 5.91% decrease of salt rejection by comparison with the virgin element. Fouling on the surface or within the pores of the membrane, oxidation, and frequency of chemical cleaning may lead to a decrease in performance of RO element [6]. RO element autopsy method was used to study the extent of membrane fouling and distribution of foulants, because it can provide precise information about foulants compositions and properties.

Table 1
Chemical compositions of the raw seawater

Main ions	mg/L
Calcium (Ca^{2+})	357.82
Magnesium (Mg^{2+})	1,142.32
Sodium (Na^{+})	9,531.64
Potassium (K^{+})	338.42
Ammonium (NH^{4+})	0.35
Barium (Ba^{2+})	0.04
Strontium (Sr^{2+})	6.99
Chloride (Cl^{-})	16,947.12
Bicarbonate (HCO_3^{-})	144.82
Sulfate (SO_4^{-})	2,636.56
Fluoride (F^{-})	1.18
Silica (SiO_2)	1.06
Boron (B^{3+})	4.23
Other parameters	
pH	7.66
TDS	46,736.43
Turbidity (NTU)	10.20

2.3. Analytical methods

The analytical techniques used in characterizing the autopsy of RO membrane include: optical microscopy, SEM-EDS, PSD analysis, XRD analysis, and XRF analysis.

2.3.1. Optical microscopes

The foulants on the membrane surface was observed by digital microscopy using a Hirox KH-8700 3D Digital microscopes for optical microscopy observation (10× and 200×). Various fractions of 12.5 cm^2 were taken from different leaves of the membrane elements for optical analysis.

2.3.2. SEM-EDS analysis

Membrane morphology and the elemental chemical analysis of the membrane samples were conducted using Phenom-XL SEM (resolution 10 nm) with energy dispersive spectrometry. The instrument was operated in low vacuum mode at chamber pressure of 60 Pa under accelerating voltage 20 kV to obtain high-quality images. Membrane sample was fixed to the specimen holder by adhesive conductive double-sided carbon tape without pretreatment or gold

Table 2
Characteristics of RO membranes applied in SWRO plant

Items	RO membrane
Manufacturer and type	Toray TM820R-440
Membrane material	Polyamide thin-film composite
Effective membrane area(m^2)	41
Water flux (L/m^2 h)	36.18
Maximum operating pressure (MPa)	8.3
Maximum operating temperature (°C)	45
Stabilized salt rejection (%)	99.8
Feed spacer(mil)	28
Continuous operation pH	2–11
Chemistry cleaning pH range	1–12
Recovery of RO system (%)	45

Table 3
Salt rejection and water flux of fouled RO element

Items	Virgin element	Fouled element
Salt rejection (%)	99.8	99.0
Water flux (L/m^2 h)	36.18	27.7

coating. The chemical component of different morphological particles was analyzed by EDS.

2.3.3. PSD analysis

The particles on the RO membrane surface were collected and dispersed in the ultrasonic disperser for 10 min. Then the PSD of the sample was measured by a laser diffraction particle size analyzer (S3500, Microtrac Inc., USA). Sample was analyzed in wet SOP and the refractive index of water was 1.33, refractive index of samples was 1.81. The software of Microtrac Flex (version 11.1.0.5) was used to analyze the data.

2.3.4. XRD analysis

In order to collect enough deposits for XRD analysis, the deposits were scrubbed carefully from three wet pieces of membrane leaves with area of 1.5 m^2 in total. Deposits mixed with deionized water like slurry was collected and filtered through a 0.45 μm cellulose acetate filters. The insoluble residue was dried at 60°C for 24 h, then was fine grinded to satisfy requirement of the particle size of XRD analysis. The deposits powder was prepared by pressing into a sample holder. A flat glass was used to press the surface of the packed powder and make it compact with the correct height and smooth surface. XRD analysis was performed with a MiniFlex600 X ray diffractometer using CuKα radiation, in the 2θ range from 3° to 90°. The power conditions were set at 40 kV/15 mA.

2.3.5. XRF analysis

XRF was employed to identify the major elements of the mineral particles on the RO membrane. The whole membrane was dried in a desiccator for 24 h, then it was clamped by a plastic jacket with the fouling layer facing down. A wavelength dispersive XRF spectrometer (Axios^{mAX}, PANalytical, Netherlands) armed with a 4 kW Rh tube was utilized. The device also equipped with PX1, PE002, and LiF200 analyzing crystals, scintillation, duplex, and P10 flow proportional counters, tube filters, and 150, 300, and 700 μm collimators. The analysis of the results was carried out using the Omnian programs, part of the SuperQ (version 5.3 A) software suite.

2.3.6. Plate and frame testing

Plate and frame testing was performed after the destructive autopsy. Round coupons were cut from the membrane of the autopsied element and placed in a plate and frame apparatus. The salt rejection and water flux of membrane was evaluated in three crossflow membrane cells connected in parallel, each with effective membrane area of 0.0028 m^2. The test conditions was 32 g/L NaCl, 55bar (25°C), surface flow rate 0.9 m/s and pH 7.01. A detailed description is given in China National Standard GB/T 32373-2015.

3. Results and discussion

3.1. Mineral particles fouling pattern

The membrane surface shown in Fig. 2 revealed that thin deposits on the membrane mostly accumulated in the parallel lines along the contact of the feed spacer with the membrane. When the deposits on the membrane were magnified, the layer of deposits consists of particles with different colors, sizes, structures, or morphologies could be observed clearly. It was noteworthy that the deposits were predominantly natural particles, which were unevenly distributed in the vicinity of feed spacer imprints and particularly between these imprints. Further observations indicated that the fouling pattern was similar at different locations of the membrane element.

Apparently the grid-like fouling pattern was formed by imprints of the feed spacer filaments which kept the membrane apart to provide flow channel. Feed spacer filaments were used to promote mass transfer and mitigate concentration polarization, which resulted in solute deposition fouling. Despite optimizing the effects of feed spacer configuration on the flow pattern could reduce fouling, it is inherently responsible for the limitation of flow zones (dead

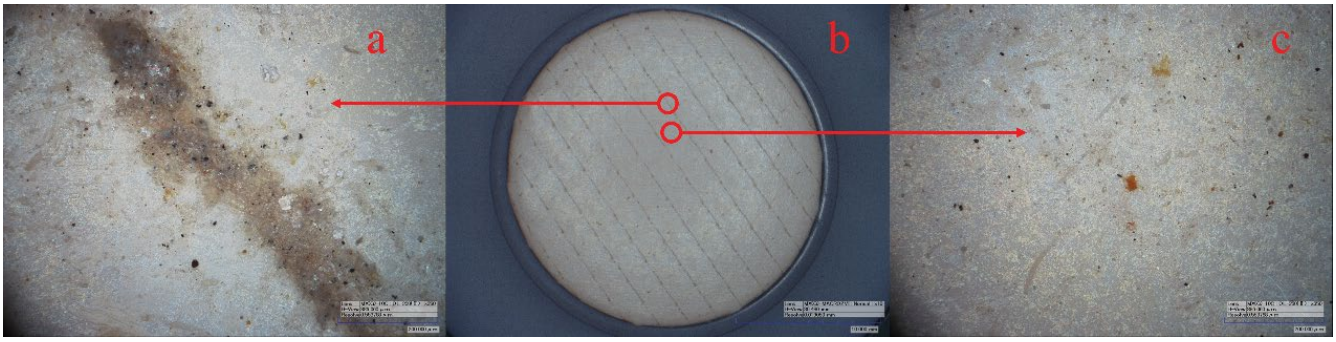

Fig. 2. Optical micrograph of deposits on the membrane surface. (a) Feed spacer filaments imprint with 350× magnification, (b) SWRO membrane with 10× magnification, and (c) zone between the feed spacer imprint with 350× magnification.

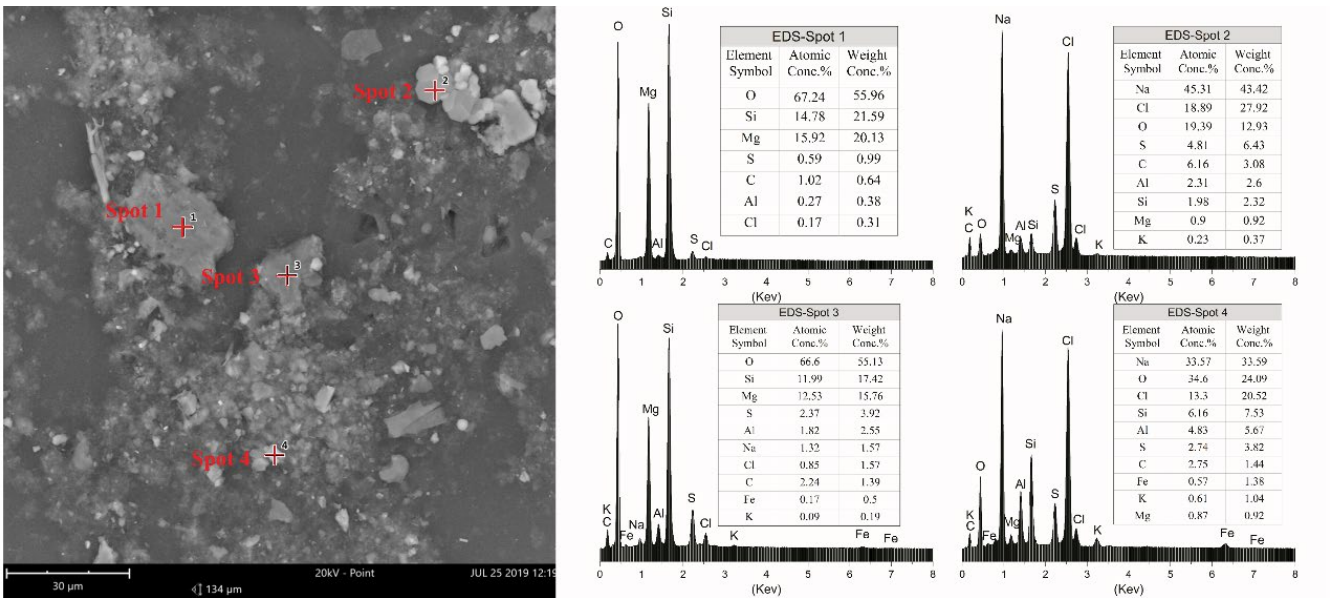

Fig. 3. SEM micrograph and associated EDS.

zones) with low shear rates leading to particles deposition fouling [5]. Recent study from three-dimensional (3D) computational fluid dynamics (CFD) simulations had demonstrated that there were low-velocity zones and stagnation zones near the spacer filaments [31]. This fouling pattern was also in agreement with the findings of Roever and Huisman [18], who observed that thin deposits on the membrane surface often concentrate in narrow zones along the contact of the feed spacer with the membrane.

The element composition of the deposits on the membrane was measured bty EDS, as exhibited in Fig. 3. The main elements in the deposits were O, Na, Cl, Si, Mg, S, Al, C, Fe, and K. Spot 1 and 3 showed the same element composition and the content of O, Si, Mg, and Al was approximately 90%, indicating that silicate minerals were the major components of the particles, which was confirmed later by the XRD analysis. Spot 2 and 4 had the highest total content of Na and Cl, indicating that the particles was NaCl, as the concentration of NaCl in seawater was high. Relatively low levels of C and Fe were also present in the deposits, suggesting that the deposits contained a few amounts of organic foulants and iron compounds [27].

3.2. PSD of mineral foulants

By analyzing the particles size distribution of minerals on the RO membrane, the ultrafiltration system integrity could be assessed indirectly on the basis of size exclusion, which is the major retention mechanism in porous membrane filtration [22].

According to Fig. 4, the mineral particle size ranged from 0.53 to 209.3 µm, and the median particle diameters (D50) of the sample was 6.46 µm. Particle size at the 10% (D10) and 90% (D90) point of the cumulative of the sample were 1.966 and 23.21 µm, respectively. The deposits had a very broad PSD (D90/D10 = 11.80), including ultrafine particles (0.1–1 µm), fine particles (1–10 µm) and medium particles (10–1,000 µm) [32]. Result of large size mineral particles deposit on the RO membrane was not in accordance with the nominal pore size of the UF membrane (20 nm). It seems that damage of the UF hollow fiber lead to the large particles got into RO membrane. These particles with diameters below 23.21 µm were cohesive due to relatively strong attractive forces between particles, meaning that they were more easily aggregated on the RO membrane than the larger particles. Thin film composite reverse osmosis (TFC-RO) membranes were known to possess characteristic ridge-and-valley structures, which enhances membrane permeability [33]. Therefore, particles deposit in the membrane valley would damage the membrane surface structure and result in further reduction of water flux.

3.3. Mineralogical analysis of particle foulants

Typical XRD patterns of RO membrane deposits are shown in Fig. 5. The patterns of reference minerals phases were taken from International Center for Diffraction Data (ICDD). Auto-flushing quantitative method with adiabatic principle was performed to calculate weight fraction of the minerals [34]. The method can be applied to samples which had no amorphous components and all the components must be fully identified. X-ray power diffractometry confirmed that the deposits were minerals with quartz, muscovite, talc, and albite with a concentration 90% in total as major phases, while minor phases were microcline, clinochlore, hematite, and amphibole with a concentration 10% in total (Table 4). The results were similar to a study on autopsy of SWRO membranes from desalination plant in Ceuta after 8 y in operation 16 [35]. The differences of pretreatment techniques used in these two plants may account for inconsistent results. These minerals on the reverse osmosis membrane surface was a result of pretreatment failure.

Most of these minerals belong to the silicate family, which consists of Si tetrahedral (SiO_4) and Al octahedral

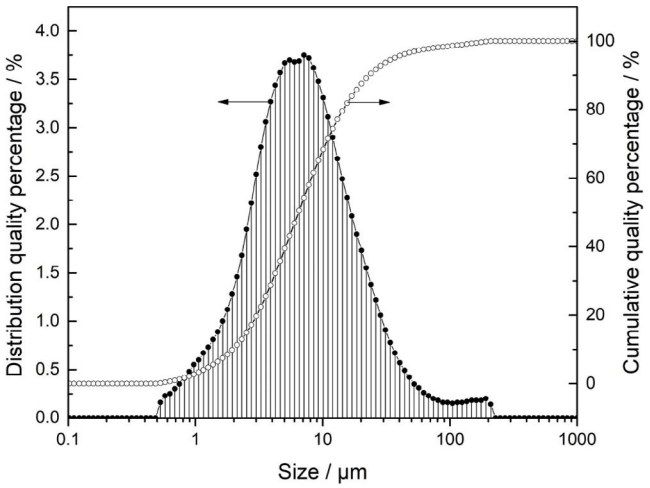

Fig. 4. Particle size distribution of membrane deposits.

($Al(OH)_2O_4$). Depending on the chemical composition of the tetrahedral and octahedral structures, mineral particles will have a permanent electrostatic negative charge at the basal surface, arising from isomorphous substitution of lattice by cations of a lower valence [26]. Therefore, the RO membrane surfaces with positively charged groups would induce rapid particles precipitation. On the other hand, at the edges of the mineral particles, the O atoms were coordinately unsaturated and pick up protons from the aqueous environment, thus forming surface OH groups. These OH groups were polar and capable of H-bonding with organic polymers and biomolecules, resulting in organic fouling or biofouling [36]. The mechanism of mineral particles fouling was critically complex and was influenced by the crystal structure, incomplete bond, surface charge, particle size and shape, membrane surface roughness and hydrophilicity, shear of drag across the membrane surface [1,24].

Mineral particles were commonly found in seawater due to weathering of silicate minerals in the earth. Most mineral particles were carried by rivers and direct ran-off to coastal waters, then deposited on the seafloor, while some micro particles were suspended in seawater which is attributed to adsorbed natural organic matter (NOM) and hydration effects at particle surfaces [20]. It was usually inevitable that mineral particles were able to pass the pretreatment filters and accumulated on the surface of reverse osmosis membrane, when the hollow fibers of ultrafiltration (UF) was broken [21,37]. The negative impacts of mineral particles fouling towards the sustainability of the desalination plants were huge. The deposits of mineral particles on the membrane surface would results in the reduction of water flux over time, adsorption of organic foulants [35], create a nutrient-enriched environment which was ideal for bacterial adhesion, adsorption of heavy metals which may accelerate the degradation of polyamide layer [26,38], frequent chemical cleaning which would damage membranes.

3.4. Cleaning of mineral particles by HF immersing

3.4.1. Effect of time on HF cleaning efficiency

The fouled membranes were cut into pieces with scale of 100 cm^2, and immersed in 2.5 wt.% solution for a specific time, at a constant temperature of 40°C. As negative controls,

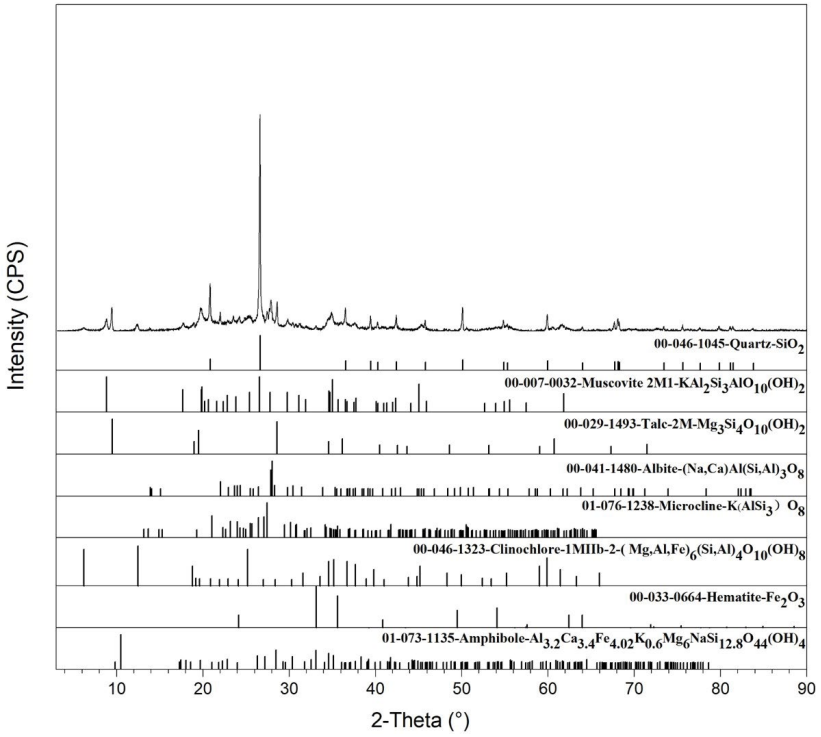

Fig. 5. X-ray powder diffraction of RO membrane deposits.

fouled membranes were immersed in deionized water. After immersing procedure, membranes were taken out of the solution and rinsed by deionized water to remove the residual cleaning agent. The remaining deposits on the membrane were examined by microscope and XRF analysis.

Cleaning time is one of the most important parameters affecting cleaning efficiency. Fig. 6 shows the effect of cleaning time on the mineral particles removal using 2.5 wt.% HF solution as cleaning agents. Most of the particles deposited on the membrane surface was dissolved gradually over the 37.5 h of immersing, while a few unreacted particles and black particles similar to inorganic carbon remained on the film surface. This phenomenon was consistent with existing report and suggested that some minerals, such as feldspar and mica, react rapidly with HF, whereas others, such as quartz, react relative slowly with HF due to the physico-chemical heterogeneity of mineral particles [25]. The fouled membrane surface elemental composition of change over time after immersing in HF solution was analyzed by XRF. Fig. 7 shows that the relative elements concentration of Na, Mg, Al, Si on the membrane surface were sharply decreased by increasing the immersing time from 0.5 to 5.5 h, then they approximately remained constant over time. These elements were consistent with the mineral composition determined by the above XRD analysis, which proves that the mineral particles were indeed dissolved by HF. It was worth noting that the sulfur concentration increased rapidly within 5.5 h, which meant the particulates on the membrane surface were removed quickly and the inherent sulfur in the membrane matrix was detected by XRF more easily. Other minor elements such as K, Ca and Fe with a relative concentration less than 0.25% in total were also reduced slightly.

3.4.2. Effect of HF immersing on membrane performance

Effect of chemical immersing on membrane performance was investigated by plate and frame testing. Although chemical cleaning could remove foulants, it may also change polyamide membrane structures, resulting in a change in permeability or salt rejection [39]. Membrane performance test results showed that the water flux of fouled membrane increased obviously, while the salt rejection of fouled membrane was decreased slightly after chemical immersing for 20 d (Fig. 8). The dropped salt rejection of the membranes may be caused by the continuous attacking of hydrogen (H^+) or hydroxide (OH^-) ions during chemical immersing,

Table 4
Results of the mineralogical analysis (XRD)

Mineral	Compound %	Classification
Quartz	35%	Tectosilicate
Muscovite	29%	Phyllosilicate
Talc	16%	Phyllosilicate
Albite	10%	Tectosilicate
Microcline	5%	Tectosilicate
Clinochlore	3%	Phyllosilicate
Hematite	1%	Oxide mineral
Amphibole	1%	Inosilicate

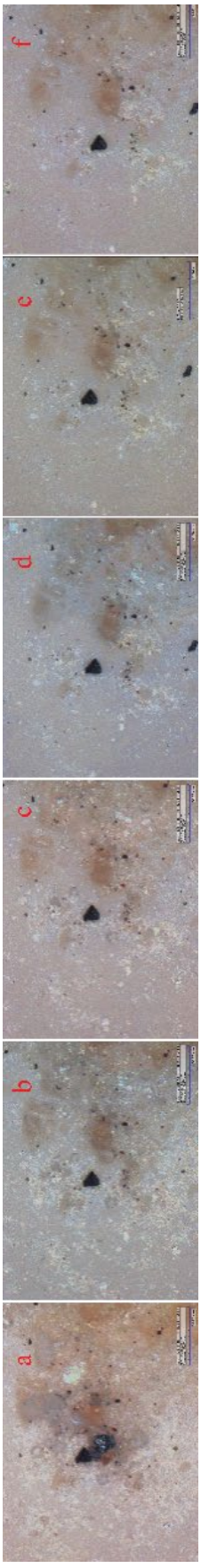

Fig. 6. Optical micrograph of fouling membrane surface immersed in HF solution (2.5% wt.) for a specific time (a) 0 h, (b) 0.5 h, (c) 1.5 h, (d) 5.5 h, (e) 13.5 h, and (f) 37.5 h.

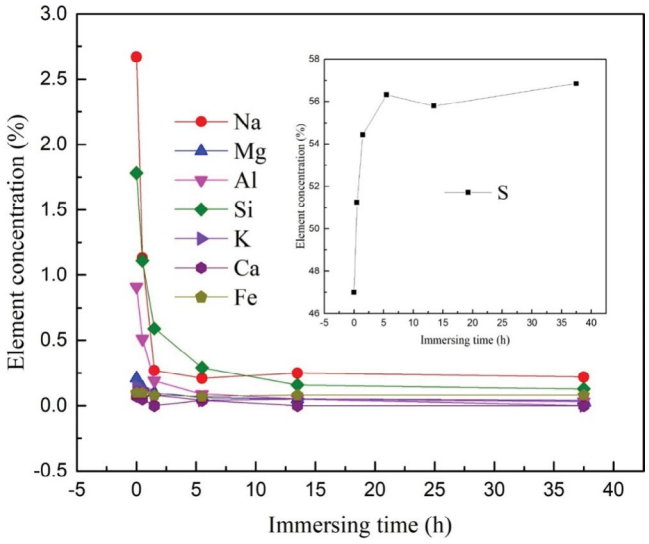

Fig. 7. Effect of immersing time on element concentration on the membrane surface

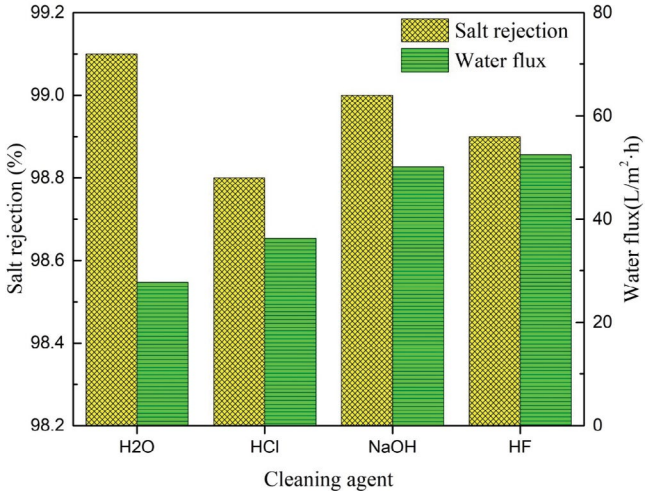

Fig. 8. Salt rejection and water flux of the membranes after 20 d immersed in cleaning agent.

which can gradually break amide polymer structures and result in enlarging the pore size of RO membrane. HCl or NaOH immersing could hardly remove the mineral particles on the RO membrane surface, but HF immersing removed most of the deposits. This indicates that membrane water flux increased by HF immersing mainly attributed to the removal of mineral deposits, whereas HCl or NaOH immersing primarily increased membrane water flux by improving membrane hydrophilicity.

4. Conclusion

In summary, a systematic investigation of the mineral particles fouling in SWRO desalination was obtained through membrane performance, fouling pattern, chemical analysis, PSD, mineralogical analysis, and chemical cleaning. The mineral particles predominantly deposit in the vicinity of feed spacer imprints and particle size ranged from 0.53 to 209.3 μm with a median particle diameters (D50) of 6.46 μm. The major phases of mineral particles were quartz, muscovite, talc, and albite with a concentration 90% in total, while minor phases were microcline, clinochlore, hematite, and amphibole with a concentration 10% in total. The representative elements of the deposits were Na, Mg, Al, Si, and could be removed effectively by 2.5 wt.% HF immersing within 5.5 h. Data from this work may be useful to assess the mineral particles fouling degree of SWRO desalination membranes, and would be especially convenient in the controlling of SWRO fouling. Moreover, it would also provide a chance to develop RO membranes with upgrade in mineral particles fouling resistance.

Acknowledgments

This work was supported by National Key R&D Program of China (2017YFC0404100), Public Science and Technology Research Funds Projects of Ocean (201505021), Special Fund for Scientific Research Institutes Basic R&D Business (K-JBYWF-2018-QR08, Y-JBYWF-2019-17).

References

[1] M. Qasim, M. Badrelzaman, N.N. Darwish, N.A. Darwish, N. Hilal, Reverse osmosis desalination: a state-of-the-art review, Desalination, 459 (2019) 59–104.
[2] X. Zheng, D. Chen, Q. Wang, Z. Zhang, Seawater desalination in China: retrospect and prospect, Chem. Eng. J., 242 (2014) 404–413.
[3] IDA Water Security Handbook 2018–2019. Media Analytics Ltd., Oxford. Available at: https://idadesal.org/dynamic-growth-for-desalination-and-water-reuse-in-2019/
[4] G. Amy, N. Ghaffour, Z. Li, L. Francis, R.V. Linares, T. Missimer, S. Lattemann, Membrane-based seawater desalination: present and future prospects, Desalination, 401 (2017) 16–21.
[5] P.S. Goh, W.J. Lau, M.H.D. Othman, A.F. Ismail, Membrane fouling in desalination and its mitigation strategies, Desalination, 425 (2018) 130–155.
[6] S.P. Chesters, N. Pena, S. Gallego, M. Fazel, M.W. Armstrong, F. del Vigo, Results from 99 seawater RO membrane autopsies, IDA J. Desal. Water Reuse, 5 (2013) 40–47.
[7] S. Jiang, Y. Li, B.P. Ladewig, A review of reverse osmosis membrane fouling and control strategies, Sci. Total Environ., 595 (2017) 567–583.
[8] Q. Liu, G.R. Xu, R. Das, Inorganic scaling in reverse osmosis (RO) desalination: mechanisms, monitoring, and inhibition strategies, Desalination, 468 (2019) 114065.
[9] T. Tong, A.F. Wallace, S. Zhao, Z. Wang, Mineral scaling in membrane desalination: mechanisms, mitigation strategies, and feasibility of scaling-resistant membranes, J. Membr. Sci., 579 (2019) 52–69.
[10] T. Miyoshi, M. Hayashi, K. Shimamura, H. Matsuyama, Important fractions of organic matter causing fouling of seawater reverse osmosis (SWRO) membranes, Desalination, 390 (2016) 72–80.
[11] W. Yin, X. Li, S.R. Suwarno, E.R. Cornelissen, T.H. Chong, Fouling behavior of isolated dissolved organic fractions from seawater in reverse osmosis (RO) desalination process, Water Res., 159 (2019) 385–396.
[12] S. Jeong, G. Naidu, T. Leiknes, S. Vigneswaran, 4.3 Membrane biofouling: biofouling assessment and reduction strategies in seawater reverse osmosis desalination, Compr. Membr. Sci. Eng., 4 (2017) 48–71.
[13] S. Nejati, S.A. Mirbagheri, D.M. Warsinger, M. Fazeli, Biofouling in seawater reverse osmosis (SWRO): impact of module geometry and mitigation with ultrafiltration, J. Water Process Eng., 29 (2019) 100782.

[14] M.T. Khan, C.L. Manes, C. Aubry, L. Gutierrez, J.P. Croue, Kinetic study of seawater reverse osmosis membrane fouling, Environ. Sci. Technol., 47 (2013) 10884–10894.
[15] X. Su, W. Li, A. Palazzolo, S. Ahmed, Permeate flux increase by colloidal fouling control in a vibration enhanced reverse osmosis membrane desalination system, Desalination, 453 (2019) 22–36.
[16] C.Y. Tang, T.H. Chong, A.G. Fane, Colloidal interactions and fouling of NF and RO membranes: a review, Adv. Colloid Interface Sci., 164 (2011) 126–143.
[17] M.W. Armstrong, S. Gallego, S.P. Chesters, Cleaning clay from fouled membranes, Desal. Water Treat., 10 (2009) 108–114.
[18] E.W.F.D. Roever, I.H. Huisman, Microscopy as a tool for analysis of membrane failure and fouling, Desalination, 207 (2007) 35–44.
[19] J. Kavitha, M. Rajalakshmi, A.R. Phani, M. Padaki, Pretreatment processes for seawater reverse osmosis desalination systems—a review, J. Water Process Eng., 32 (2019) 100926.
[20] J.K. Edzwald, J. Haarhoff, Seawater pretreatment for reverse osmosis: chemistry, contaminants, and coagulation, Water Res., 45 (2011) 5428–5440.
[21] M. Badruzzaman, N. Voutchkov, L. Weinrich, J.G. Jacangelo, Selection of pretreatment technologies for seawater reverse osmosis plants: a review, Desalination, 449 (2019) 78–91.
[22] T. Krahnstöver, R. Hochstrat, T. Wintgens, Comparison of methods to assess the integrity and separation efficiency of ultrafiltration membranes in wastewater reclamation processes, J. Water Process Eng., 30 (2019) 100646.
[23] S.G.S. Rodriguez, N. Sithole, N. Dhakal, M. Olive, J.C. Schippers, M.D. Kennedy, Monitoring particulate fouling of North Sea water with SDI and new ASTM $MFI_{0.45}$ test, Desalination, 454 (2019) 10–19.
[24] R.A. Schoonheydt, C.T. Johnston, F. Bergaya, 1 - Clay minerals and their surfaces, Dev. Clay Sci., 9 (2018) 1–21.
[25] N. Li, F.B. Zeng, J. Li, Q. Zhang, Y. Feng, P. Liu, Kinetic mechanics of the reactions between HCl/HF acid mixtures and sandstone minerals, J. Nat. Gas Sci. Eng., 34 (2016) 792–802.
[26] B. Baeyens, M.M. Fernandes, 5 - Adsorption of heavy metals including radionuclides, Dev. Clay Sci., 9 (2018) 125–172.
[27] N.M. Martel, J.J. Sadhwani, S. Malamis, M.O. Petropoulou, Structural and chemical characterization of long-term reverse osmosis membrane fouling in a full scale desalination plant, Desalination, 305 (2012) 44–53.
[28] M. Karime, S. Bouguecha, B. Hamrouni, RO membrane autopsy of Zarzis brackish water desalination plant, Desalination, 220 (2008) 258–266.
[29] S.S. Madaeni, S. Samieirad, Chemical cleaning of reverse osmosis membrane fouled by wastewater, Desalination, 257 (2010) 80–86.
[30] J.Y. Yang, Y.S. Li, B. Huang, Research on refurbishing of the used RO membrane through chemical cleaning and repairing with a new system, Desalination, 320 (2013) 49–55.
[31] B. Gu, C.S. Adjiman, X.Y. Xu, The effect of feed spacer geometry on membrane performance and concentration polarisation based on 3D CFD simulations, J. Membr. Sci., 527 (2017) 78–91.
[32] H.G. Merkus, Particle Size Measurements: Fundamentals, Practice, Quality, Springer Science & Business Media, 2008, pp. 1–11.
[33] X. Song, B. Gan, Z. Yang, C.Y. Tang, C. Gao, Confined nanobubbles shape the surface roughness structures of thin film composite polyamide desalination membranes, J. Membr. Sci., 582 (2019) 342–349.
[34] F.H. Chung, Quantitative interpretation of X-ray diffraction patterns of mixtures. II. Adiabatic principle of X-ray diffraction analysis of mixtures, J. Appl. Crystallogr., 7 (1974) 526–531.
[35] G.F. Álvarez, G. Garralón, F. Plaza, A. Garralón, J. Pérez, M.A. Gómez, Autopsy of SWRO membranes from desalination plant in Ceuta after 8 years in operation, Desalination, 263 (2010) 264–270.
[36] S.V. Churakov, X. Liu, 3 – Quantum-chemical modelling of clay mineral surfaces and clay mineral–surface–adsorbate interactions, Dev. Clay Sci., 9 (2018) 49–87.
[37] C. Xin, J. Wang, H. Jia, H. Wen, J. Li, Hollow fiber membrane integrity warning device based on laser extinction particles detection technology, Sep. Purif. Technol., 224 (2019) 295–303.
[38] O. Ferrer, O. Gibert, J.L. Cortina, Reverse osmosis membrane composition, structure and performance modification by bisulphite, iron(III), bromide and chlorite exposure, Water Res., 103 (2016) 256–263.
[39] T. Fujioka, S.J. Khan, J.A. McDonald, A. Roux, Y. Poussade, J.E. Drewes, L.D. Nghiem, N-nitrosamine rejection by reverse osmosis: effects of membrane exposure to chemical cleaning reagents, Desalination, 343 (2014) 60–66.